Alistair J. Standish, Jonathan J. Whittall and Renato Morona
Tyrosine phosphorylation enhances activity of pneumococcal autolysin LytA
Microbiology, 2014; 160(12):2745-2754.

Microbiology Papers in Press. Published October 6, 2014 as doi:10.1099/mic.0.080747-0

Tyrosine phosphorylation enhances activity of pneumococcal autolysin LytA

Running Title: LytA tyrosine phosphorylation enhances choline binding and amidase activity

Contents: Microbial Pathogenicity

Alistair J. Standish[#], Jonathan J. Whittall and Renato Morona

School of Molecular and Biomedical Sciences, University of Adelaide, SA, Australia, 5005.

Please address correspondence to: Alistair Standish (Ph: +61 8 8313 0232; Fax: +61 8 8313 753; :alistair.standish@adelaide.edu.au).

Word count:

Summary - 218

Main Text – 5298

Tables – 1

Figures - 7

Summary

For a long time tyrosine phosphorylation has been recognized as a crucial post translational regulatory mechanism in eukaryotes. However, only in the past decade has recognition been given to the crucial importance of bacterial tyrosine phosphorylation as an important regulatory feature of pathogenesis. This study describes the effect of tyrosine phosphorylation on the activity of a major virulence factor of the pneumococcus, the autolysin LytA, and a possible connection to the *Streptococcus pneumoniae* capsule synthesis regulatory proteins (CpsB, CpsC & CpsD). We show that *in vitro* pneumococcal tyrosine kinase, CpsD, and the protein tyrosine phosphatase, CpsB, act to phosphorylate and dephosphorylate LytA. Furthermore, this modulates LytA function *in vitro* with phosphorylated LytA binding more strongly to the choline analogue DEAE. A phospho-mimetic (Y264E) mutation of the LytA phosphorylation site displayed similar phenotypes as well as an enhanced dimerization capacity. Similarly, tyrosine phosphorylation increased LytA amidase activity, as evidenced by a turbidometric amidase activity assay. Similarly, when the phospho-mimetic mutation was introduced in the chromosomal *lytA* of *S. pneumoniae*, autolysis occurred earlier and at an enhanced rate. This study thus describes to our knowledge the first functional regulatory effect of tyrosine phosphorylation on a non-capsule related protein in the pneumococcus, and suggests a link between the regulation of LytA-dependent autolysis of the cell, and the biosynthesis of capsular polysaccharide.

Introduction

Tyrosine phosphorylation is rapidly becoming a major focus of bacterial research, with studies illustrating its critical link to bacterial pathogenicity (Standish & Morona, 2014; Whitmore & Lamont, 2012). Indeed, we have been amongst those showing a link, with our long interest in the role of bacterial tyrosine kinase (BY-Kinase) CpsD and protein tyrosine phosphatase (PTP) CpsB in the regulation of capsule synthesis in the major human pathogen, *Streptococcus pneumoniae*, and as a novel target for the development of antimicrobials (Byrne *et al.*, 2011; Ericsson *et al.*, 2012; Morona *et al.*, 2000; Morona *et al.*, 2002; Morona *et al.*, 2006; Standish *et al.*, 2012; Standish *et al.*, 2013). However, we are also interested in whether tyrosine phosphorylation plays roles outside the capsule biogenesis, regulating the function of various proteins via specific tyrosine phosphorylation.

Since early last century, the pneumococcus has been recognized to possess a characteristic autolysis induced during the stationary phase of growth (Goebel & Avery, 1929). This has since been shown to be caused by the product of the *lytA* gene, a N-acetylmuramoyl L-alanine amidase (Garcia *et al.*, 1985). LytA belongs to a family of proteins known as choline binding proteins (CBP) (Rosenow *et al.*, 1997), which while having diverse functions all share the ability to bind phosphorylcholine residues present in the pneumococcal cell wall (Rosenow *et al.*, 1997). For LytA, binding to choline is essential for its amidase activity. LytA resides in the cytoplasm in the inactive E-form, with binding to choline present in the cell wall (Giudicelli & Tomasz, 1984), and subsequent dimerization, resulting in formation of the C-form which possesses functional amidase activity. The structure of the choline binding

domain of LytA has illustrated that it contains a total of 6 choline binding repeats, which are characteristic of CBPs, along with a total of 4 choline binding sites (**Fig. 1**) (Fernandez-Tornero *et al.*, 2001; Fernandez-Tornero *et al.*, 2002). Unlike other CBPs, LytA does not possess a signal sequence, and to date it is unknown how it translocates to the cell wall, in order to bind phosphorylcholine and hydrolyse the cell wall.

The exact role of LytA in *S. pneumoniae* physiology is still unclear, with some suggestion that it is required for the release of the toxin pneumolysin (Martner *et al.*, 2008), as well as contributing to bacterial fractricide (Eldholm *et al.*, 2009). However, while its function is still debated, it is recognized as a virulence factor, with mutation resulting in decreased ability to cause disease in *in vivo* models (Berry & Paton, 2000; Dalia & Weiser, 2011).

A recent study on the phosphoproteome of *S. pneumoniae* identified LytA as one of 12 proteins phosphorylated on tyrosine (Sun *et al.*, 2010). With CpsD the only BY-kinase identified to date in *S. pneumoniae*, and both proteins known to localize to the cell septum (Henriques *et al.*, 2011; Mellroth *et al.*, 2012), we hypothesized that CpsD plays a role in the phosphorylation of LytA, and that phosphorylation regulates its amidase activity. This study shows for the first time an effect of tyrosine phosphorylation on protein function in *S. pneumoniae* encoded outside of the capsule locus, and provides a hitherto unidentified link between cell autolysis and capsular polysaccharide biosynthesis.

Methods

Growth media and growth conditions

S. pneumoniae strains (listed in Table 1) were routinely grown in Todd-Hewitt broth with 1% Bacto yeast extract (THY) or C+Y (McAllister *et al.*, 2004) at 37°C as indicated or on Columbia Blood Agar plates supplemented with 5% (v/v) horse blood and grown at 37°C in 5% CO_2. Broth cultures were grown at 37°C without aeration. *E. coli* cultures were grown in LB at 37°C with aeration. Antibiotics were used at the following concentrations: *E. coli*; Ampicilin 100 µg/ml, Erythromycin 500 µg/ml; *S. pneumoniae*: Erythromycin 0.2 µg/ml, Streptomycin 150 µg/ml, Kanamycin 200 µg/ml.

DNA methods and *E. coli* transformation

E.coli K-12 DH5α was used for all cloning. DNA manipulation, PCR, and transformation into *E.coli* were performed as previously described (Morona *et al.*, 1995).

Protein purification

LytA was purified essentially as described previously (Romero *et al.*, 2007). Briefly, overnight cultures of the indicated strain were pelleted, washed in 20 mM phosphate buffer pH 7, and lysed at > 1000 PSI via a French Pressure cell. Insoluble material was removed by ultracentrifugation (150,000 × *g* for 1 hr) and isolated soluble fractions incubated with DEAE Sepharose Fastflow (GE Healthcare) for 1 hr at room temperature. DEAE Sepharose was washed three times in 20 mM phosphate buffer pH 7.0 supplemented with 1.5 mM NaCl. LytA was then eluted from DEAE Sepharose with 20 mM phosphate buffer pH 7 with 2% (w/v) choline chloride. The

purity of eluted LytA was confirmed as > 95% by SDS-PAGE, and LytA was stored at - 20 °C either with or without dialysis in 50 mM Phosphate buffer pH 7.0. For analysis of LytA purified from DH5α containing pGL80 and pCpsCD, the protein was washed using Amicon Ultra-4 centrifugal filter units and resuspended in 50 mM phosphate buffer without choline and NaCl. Protein estimation was carried out using BCA Kit (ThermoFisher). CpsB was purified as previously described (Standish *et al.*, 2012).

Construction of amino acid substitutions in LytA

Tyrosine 264 of LytA in pGL80 was mutated to Phenylalanine (Oligonucleotides AS95, AS96), Glutamate (AS97, AS98), and Alanine (AS99, AS100) using the QuikChange Lightning Site Directed Mutagenesis Kit® (Stratagene) according to the manufacturer's instructions. Mutational alterations were confirmed by DNA sequencing.

Antibody production

In order to produce antibodies against LytA and CpsB, purified protein (≥ 95 % as judged by Coomassie stained SDS-PAGE) was supplied to IMVS, Veterinary Services, Gilles Plain SA, Australia where polyclonal antibody was produced in rabbits. αLytA recognizes all variants of LytA described here with equal efficiency, as determined by comparing Western immunoblots with αLytA with Coomassie Brilliant Blue stained SDS-PAGE analysis (data not shown).

Construction of LytA amino acid substitutions in *S. pneumoniae* D39.

To construct point mutations within *lytA*, first the Janus cassette (Sung *et al*., 2001) was inserted into the *lytA* gene using overlap extension PCR. The 5' region of *lytA* was amplified with AS117 + AS101, a 3' region with AS118 + AS102 and the Janus cassette with AS113 + AS114. These PCR products were then combined in a second round of PCR with AS101 and AS102. Overlap product was then transformed into a Streptomycin resistant ($Strep^R$) D39 strain (D39S), which was made resistant by transformation with a PCR product of *rpsL* from $Strep^R$ Rx1. Transformants were selected on the basis of Kanamycin resistance, and Streptomycin sensitivity, and confirmed by sequencing.

LytA was mutated using overlap PCR using the following combination of oligonucleotides for 5' and 3' regions of *lytA* containing the relevant mutation;Y264F: AS101 + AS95, AS102 +AS96; Y264E: AS97 +AS101, AS102 + AS98; Y264A: AS101 + AS99. The original PCR products were then combined in a second round of PCR using AS101 and AS102 and transformed into D39 LytAJanus, and $Strep^R$ colonies selected for. Mutations were confirmed by sequencing. Transformations were carried out as described previously (Standish *et al.*, 2005).

LytA Binding Assays

In order to investigate affinity of LytA to the choline analogue DEAE (DEAE sepharose fast flow – GE Healthcare Life Sciences), 500 µl of 0.2 mg/ml of soluble lysate from the indicated *E. coli* strain was incubated with 20 µl of DEAE Sepharose for 10 mins while rotating at room temperature. DEAE was then washed in 50 mM phosphate buffer pH 7.0 with 1.5 M NaCl × 3 and subsequently resuspended in 2 ×

sample buffer, and amount of LytA present analyzed by Coomassie Brilliant Blue staining of the SDS-PAGE gel.

Construction of pCpsCD

For the BY-kinase CpsD to be active it requires the polysaccharide co-polymerase protein, or kinase adaptor membrane protein, CpsC (Bender & Yother, 2001). In, *S. aureus* fusion of the C-terminal cytoplasmic region of this homologous protein to the BY-kinase results in an active protein (Olivares-Illana *et al.*, 2008; Soulat *et al.*, 2006) We hypothesized this would also be the case in *S. pneumoniae*. Therefore, we fused D202-K230 of Cps4C(SP_0348) (the predicted C-terminal cytoplasmic region) to Cps4D (SP_0349) by overlap PCR. Originally we amplified D202-K230 of Cps4C with AS1 and AS2 and Cps4D with AS3 and AS4. These products were then combined in a second round of PCR and amplified with AS1 and AS4. This PCR product was ligated into pGEMT-Easy (Promega). Oligonucleotides AS68 and AS77 (Table 1) were used to amplify the DNA sequence and this PCR product then cloned into pAL2 (Beard *et al.*, 2002) with the *lux* operon deleted, as described previously (Trappetti *et al.*, 2011). Transformant of E. *coli* DH5α containing the plasmid (pCpsCD) was confirmed by PCR and sequencing.

SDS-PAGE and Western immunoblot

Proteins were separated on 12% SDS-PAGE as previously described (Laemmli, 1970) using low molecular weight marker (Amersham). For Western immunoblot samples were transferred to either Immobilon-P (Millipore) (αPY; PY-20 - Santa Cruz Biotechnology), or Nitrobind (GE Water and Process Technologies) (α-LytA). Membranes were probed with primary antibody overnight and after washes incubated

as appropriate with either horseradish peroxidase-conjugated goat anti-rabbit or goat anti-mouse secondary antibodies (Biomediq DPC) for 2 h. The membrane was then incubated with chemiluminescence blotting substrate (Sigma) for 5 min, followed by exposure of the membrane to X-ray film (Agfa). The film was developed using a Curix 60 automatic X-ray film processor (Agfa) or imaged with a Kodak Image Station 4000MM Pro (Carestream Molecular Imaging) to visualize the reactive bands.

Non-denaturing PAGE

Non-denaturing PAGE was undertaken essentially as for SDS-PAGE, but with SDS omitted from all steps, including the PAGE, Running buffer, and the 2 × Sample buffer. 12 % Gels were electrophoresed at 120V at 4°C, and stained with Coomassie Brilliant Blue.

Turbidometric amidase activity assay. Amidase activity was analyzed by measuring the decrease in turbidity of D39 LytAJanus (Table 1) cells after incubation with purified LytA proteins, essentially as described previously (Mellroth *et al.*, 2014). D39 LytAJanus was grown to $OD_{600} \approx 0.5$ in THY, then pelleted by centrifugation, washed twice in PBS and stored at -20 °C in PBS until use. In order to measure specific activity, thawed cells were equilibrated to $OD_{600} \approx 1.0$ and distributed into wells. They were then incubated with either 2 $\mu g/ml^{-1}$ purified protein or 250 $\mu g/ml^{-1}$ of respective cell lysates. The initial rate of decrease in turbidity was determined for each protein, and their relative activities were calculated compared to the wt control. Results for purified proteins and cell lysates are from 2 and 3 independent experiments respectively.

Growth Curves

For growth curves, *S. pneumoniae* were taken from Blood Agar plates incubated for 18 h at 37°C in 5% CO_2, and inoculated into THY and grown till mid-log phase ($OD_{600} \approx 0.5$). Bacteria were then sub-cultured 1/20 into C+Y and incubated at 37°C in 96 well tray covered with Breath Easy® membrane (Sigma) in Powerwave XS (Biotek). A_{600} readings were taken every 30 min for the indicated time period. Rate of autolysis was determined by comparing the fastest rate of autolysis in each strain over a 1 hr time period. The results are represented as % of the wt. Results are from 4 separate experiments, with each experiment performed at least in duplicate.

Results

LytA is tyrosine phosphorylated on Y264 by CpsD and dephosphorylated by CpsB

A recent report on the phosphoproteomic profile of *Streptococcus pneumoniae* D39 (Sun *et al.*, 2010) identified the autolysin, LytA, as being tyrosine phosphorylated on Y264. As we have investigated the role of the tyrosine phospho-regulatory system CpsBCD in the regulation of capsule biosynthesis (Byrne *et al.*, 2011; Morona *et al.*, 2000; Morona *et al.*, 2002; Morona *et al.*, 2004; Morona *et al.*, 2006; Standish *et al.*, 2012), we hypothesized that this system may directly influence the level of tyrosine phosphorylation of the autolysin LytA, as to date no other BY-kinases have been described in the pneumococcus (Morona *et al.*, 2000). Thus, we hypothesized that CpsD is responsible for tyrosine phosphorylation of LytA. In order to investigate this, we constructed a fusion comprising the C-terminal cytoplasmic portion of CpsC (D202-K230), which is required for CpsD activity, and full length CpsD in the vector pAL2 (Beard *et al.*, 2002) as described in the Materials and Methods. This was based on previous work undertaken on homologous proteins in *S. aureus* (Olivares-Illana *et al.*, 2008). When this this plasmid (pCpsCD) was transformed into DH5α, we noticed that hyper phosphorylation occurred indicating that the kinase was active (**Fig. 2a**). Thus, we transformed pCpsCD together with a plasmid encoding LytA (pGL80) into DH5α (Garcia *et al.*, 1986), and purified LytA. LytA purified from this strain (LytA-P) as described in Materials and Methods had higher levels of phosphorylation compared to LytA from control strain containing vector alone, suggesting CpsD can phosphorylate LytA (**Fig. 2b, lanes 1 & 2**).

Sun et al. (2010) (Sun *et al.*, 2010) reported that LytA was phosphorylated on Tyrosine 264 (**Fig. 1a**). To confirm this finding we mutated this tyrosine to a phenylalanine. Purification of this protein from a strain also containing pCpsCD yielded $LytA_{Y264F}$ which reacted weakly with αPTyr, similar to wt LytA when purified from a strain lacking pCpsCD (**Fig. 2b**). This suggests that Tyrosine 264 is the primary residue phosphorylated by CpsCD.

In order to investigate if the PTP CpsB can act on LytA-P, purified LytA-P (from *E. coli* DH5α containing pGL80 and pCpsCD) was incubated with purified CpsB and the level of tyrosine phosphorylation investigated by Western immunoblotting (**Fig. 2c**). Incubation with CpsB decreased phosphorylation by approximately 90% suggesting the PTP can de-phosphorylate LytA-P. Thus, this data suggested that the capsule regulatory proteins CpsB and CpsD may play a role in LytA phosphorylation.

LytA Tyrosine phosphorylation enhances binding of LytA to choline analogue DEAE

As Y264 is hypothesized to play a role in the affinity of LytA to choline, we investigated the ability of LytA, LytA-P, and $LytA_{Y264F}$-P in *E. coli* derived soluble protein fractions to bind DEAE, the choline analogue utilized to purify the autolysin. As well as being a useful method for easily purifying LytA, DEAE has been shown to result in conversion of LytA to the active E-form at similar concentrations to choline (Sanz *et al.*, 1988). We first confirmed that LytA (lane 1), LytA-P (lane 2), and $LytA_{Y264F}$-P (lane 3) were present in the lysates at the same level (**Fig. 3a**). Then, we

incubated lysates with DEAE-Sepharose, and investigated LytA binding by SDS-PAGE and Coomassie Blue staining. LytA-P was detected at approximately 1.6 fold higher levels than LytA (lane 1 vs lane 2) (**Fig. 3b & 3c**). Furthermore, $LytA_{Y264F}$-P bound at a similar level to LytA (lane 1 vs lane 3), suggesting specific phosphorylation of Y264 enhanced binding to DEAE.

In order to further confirm the specific effects of phosphorylation of Y264, a phospho-mimetic substitution was also constructed ($LytA_{Y264E}$). In order to control for the change in size of the residue, we also constructed a control mutation ($LytA_{Y264A}$). Investigation using Phyre2 suggested that these mutations would not influence the secondary structure of the protein (Kelley & Sternberg, 2009). Furthermore, the stability of all proteins was investigated by limited proteolysis and were similar to the wild-type protein (data not shown).

Incubation of the lysates of containing these proteins with DEAE showed results which mirrored those seen with LytA and LytA-P. The phospho-mimetic mutation ($LytA_{Y264E}$; lane 2) enhanced affinity to DEAE while the phospho-ablative mutation ($LytA_{Y264A}$; lane 3) was less than the wt control (lane 1) (**Fig. 4b & 4c**). Thus, this provided further evidence that it is specifically the tyrosine phosphorylation of Y264 which is responsible for the increased affinity.

Phosphorylation modulates LytA dimerization

The purification of LytA as described in the Materials and Methods relies on the affinity of the amidase to choline, and thus this method purifies the C-form or active form of the enzyme. When we separated the LytA protein on non-denaturing PAGE in

order to investigate their native oligomeric conformation, in all cases a single band was present. The C-form of LytA is dimeric (Fernandez-Tornero *et al.*, 2001), and thus we reasoned that this band represents the dimeric form of the protein (**Fig. 5a**). We hypothesised that as $LytA_{Y264E}$ had increased affinity to choline, it would show an increased ability to retain its dimeric form when choline was removed by dialysis. We thus undertook dialysis in 50 mM phosphate buffer pH 7.4 and used non-denaturing-PAGE to assess the oligomeric state of LytA. Consistently we saw that $LytA_{Y264E}$ retained the higher order oligomeric state to a greater level than the wt, $LytA_{Y264F}$ or $LytA_{Y264A}$ (**Fig. 5a & 5b**). Separation of the proteins post dialysis on denaturing SDS-PAGE resulted in one band for each LytA variant (**Fig. 5c**). Addition of choline resulted in only one band again being visible on the non-denaturing PAGE (data not shown). Thus, this suggested $LytA_{Y264E}$ had an increased ability to retain the dimeric form during dialysis. This provided further confirmation that $LytA_{Y264E}$ substitution increased affinity to choline which is essential for LytA dimerization.

Tyrosine phosphorylation increases LytA Amidase activity

As tyrosine phosphorylation of LytA increased affinity to choline, and the ability of LytA to dimerise, we reasoned this may also enhance LytA amidase activity. In order to investigate this, we utilised a turbidometric amidase activity assay as described in the materials and methods. First, we utilized purified proteins of the different LytA forms to investigate activity. However, no significant differences were apparent between the strains (**Fig. 6a**). We hypothesized that this was due to the fact that the enzymes had already undergone the “conversion” process of pneumococcal amidases, ; the proteins were purified by elution with 2 % choline, and thus would already be converted into the C-form.

Thus, in order to investigate amidase activity prior to the conversion process, we used cell lysates containing LytA, as the proteins were present in lysates at equal levels (**Fig. 3a & 4a**). These would contain LytA in the inactive E-form, as they had not been converted by binding to choline or a choline analogue. The control strain, DH5α containing vector alone, led to only minimal decrease in turbidity of D39LytAJANUS (approximately 10% of the wild-type control). LytA-P had 215% of wildtype activity, with this increase lost in $LytA_{Y264F}$-P (**Fig. 6b**). Similarly, phospho-mimetic substitution of LytA (LytAY264E) had increased activity, while the phospho-ablative mutation did not. Thus, this data suggested phosphorylation of Y264 results in increased LytA conversion capacity likely through increasing capacity to bind choline.

Chromosomal mutation of Y264 alters autolysis of *S. pneumoniae*

As *in vitro* we had seen that phosphorylation of LytA, and phospho-ablative mutation altered the activity of LytA, we were interested to see whether this effect would be evident in *S. pneumoniae*. Thus, we constructed *S. pneumoniae* D39 mutants expressing chromosomally encoded LytA with phospho-ablative (D39$LytA_{Y264F}$; D39$LytA_{Y264A}$) and phospho-mimetic (D39$LytA_{Y264E}$) mutations as described in the Materials and Methods. These strains had similar levels of LytA, as determined by Western immunoblotting (**Fig. 7a**). We then investigated the growth of these strains over an extended length of time in C+Y. During logarithmic growth, there was no apparent difference in growth (**Fig. 7b**). However, consistently, the strain with the phospho-ablative mutation (D39$LytA_{Y264F}$) showed a prolonged time to lysis compared to the wt. Conversely, the strain with the phospho-mimetic mutation (D39$LytA_{Y264E}$) showed an earlier onset of autolysis. The strain with the additional

control mutation (D39LytA$_{Y264A}$) was similar to the wt. When we compared the rate of autolysis of the strain by comparing the slope of lysis, we saw that the phospho-mimetic mutation led to a significant increase in the rate of autolysis, with this significantly different from other strains (**Fig. 7c**). Thus, these results suggest that tyrosine phosphorylation of LytA on Y264 enhances activation of LytA activity in *S. pneumoniae*.

Discussion

This is the first study to our knowledge to describe tyrosine phosphorylation as a regulator of non-capsule related protein function in the major human pathogen *Streptococcus pneumoniae*. Furthermore, with the only pneumococcal BY-kinase found to date the key capsule regulator CpsD (Morona *et al.*, 2000), it seems possible that regulation of capsule and LytA activity is linked. Indeed, we have shown CpsD, as well as pneumococcal PTP CpsB, can act on LytA as a substrate *in vitro*, although as yet we have been unable to detect this *in situ*, likely due to low levels of LytA tyrosine phosphorylation. Previous studies illustrated that LytA as well as CpsD and BY-kinase adaptor protein CpsC locate to the septa of *S. pneumoniae* (De Las Rivas *et al.*, 2002; Henriques *et al.*, 2011; Mellroth *et al.*, 2012), suggesting the possibility that these proteins co-localize, further suggestive of a link between capsular polysaccharide synthesis and autolysis.

Sun *et al*. recently performed a phosphoproteomic study of the pneumococcus in which they showed that Y264 of LytA was phosphorylated (Sun *et al.*, 2010). We have confirmed this finding, showing that this is the predominant site of phosphorylation. LytA is comprised of two distinct domains, an N-terminal domain responsible for the N-acetyl muramyl amidase activity, and a C-terminal choline binding domain, responsible for the ability of LytA to bind to phosphorylcholine residues present in the cell wall. Y264 is present in C-terminal choline binding domain within Choline Binding Repeat 4. Indeed, it has been suggested that this residue is important for the binding of choline (**Fig. 1a & 1b**) (Fernandez-Tornero *et al.*, 2002). While there is significant homology between the ChBRs, Y264 is the only tyrosine at this particular site.

The forces responsible for the binding of the choline in the family of CBPs are the same in all cases. While one component is hydrophobic, another is electrostatic, a cation-π interaction between the electron-rich systems of aromatic rings and the positive charge of the choline (Fernandez-Tornero *et al.*, 2001). We hypothesized that the increased negative charge of phosphorylation at Y264 may be important for the binding of LytA to phosphorylcholine, and regulation of its subsequent amidase activity, and thus set out to investigate this.

We showed that tyrosine phosphorylation increased the affinity of LytA to the choline analogue DEAE-Sepharose. Furthermore, these affects were largely prevented by phospho-ablative substitution ($LytA_{Y264F}$). Thus, this suggested that specific phosphorylation of Y264 was responsible for this increase in affinity. Additionally, phospho-mimetic substitution ($LytA_{Y264E}$) also showed increased affinity to DEAE-Sepharose, while the corresponding control ($LytA_{Y264A}$) did not, further supporting our observations.

In the cytoplasm, LytA resides in the inactive E-form, with the protein in the monomeric state (Tomasz & Westphal, 1971). Conversion to the catalytically active C-form occurs following interaction with phosphoryl-choline in the cell wall, resulting in subsequent LytA dimerization. While conversion and dimerization are different processes, it is still not known whether conversion can only occur following the formation of the dimer (Romero *et al.*, 2007). Our analysis of the oligomeric state of the LytA protein following dialysis, suggested that the phospho-mimetic form

412 ($LytA_{Y264E}$) retain its dimeric state to a greater extent than the wild-type and phospho-
413 ablative forms ($LytA_{Y264F}$ & $LytA_{Y264A}$), which correlates with an increased affinity to
414 choline. Furthermore, we also showed that this correlated with a difference in the
415 overall activity of the enzyme. Interestingly, when we used purified proteins, having
416 already undergone conversion due to the purification process, there were no
417 significant amidase activity differences between the proteins (**Fig. 6a**). This provides
418 evidence that we have not affected the secondary structures of the proteins through
419 mutation or phosphorylation, as they still possess the same activity when bound to
420 choline. However, when we used *E. coli* soluble cell lysates, in which LytA had not
421 undergone previous conversion, significant differences were evident (**Fig. 6b**).
422 Phosphorylation of Y264 enhanced LytA amidase activity, likely due to an increased
423 capacity to bind choline and undergo the conversion to the C-form.
424
425 In order to confirm that this *in vitro* phenomenon played a role *in vivo*, we constructed
426 LytA phospho-ablative and phospho-mimetic mutations in *lytA* on the chromosome of
427 *S. pneumoniae* D39. The phospho-ablative substitution, $D39LytA_{Y264F,}$ showed
428 prolonged time to lysis compared to the isogenic wt, suggestive that phosphorylation
429 was occurring on the wt LytA in order to promote autolysis. Furthermore, the strain
430 with the phospho-mimetic ($D39LytA_{Y264E}$) substitution showed an earlier onset of
431 autolysis. Additionally, by comparison of the slope of lysis, it was evident that the
432 phosphomimetic mutation led to an increased autolytic capability, correlating with our
433 *in vitro* results. Thus, this data suggested that phosphorylation was responsible for
434 both an earlier onset, and faster autolysis phase.
435

While LytA was originally postulated to be always situated in the cell wall, in recent times evidence has emerged suggesting LytA is located in the cytoplasm until the membrane is disrupted and the protein is able to gain access to peptidoglycan and cause the cell to undergo autolysis (Mellroth *et al.*, 2012). Such a model, which seems likely, would suggest that no regulation mechanism is required. However, our work showed that phospho-mimetic and phospho-ablative mutations on the chromosome of the pneumococcus altered the time to autolysis in whole cell pneumococci, suggesting LytA tyrosine phosphorylation may alter the process whereby LytA gains access to its substrate. This may contribute *in vivo* to the numerous roles that LytA plays, such as in bacterial fractricide, release of pneumolysin and the control of bacterial size.

With LytA a member of the of the CBP family in *S. pneumoniae*, it is interesting to speculate whether other CBPs in the pneumococcus whose affinity for choline are affected by tyrosine phosphorylation in a similar way to LytA. Indeed, another CBP, CbpC is also phosphorylated on tyrosine, although this phosphorylation does not occur in the region of the choline binding domain of the protein, and thus its effect on function is less clear (Sun *et al.*, 2010). Furthermore, LytA is also known to be phosphorylated on Threonine (Sun *et al.*, 2010), with further work required to determine whether this affects LytA function.

Additionally, we are interested in investigating further correlations between the phosphotyrosine regulatory system and LytA. Previous data has suggested that loss of capsule has an effect on the sensitivity of the pneumococcus to LytA amidase activity (Fernebro *et al.*, 2004). With deletion of either the BY-kinase CpsD or PTP CpsB resulting in strains possessing reduced capsule, this approach will be problematic.

When we expressed the active CpsCD (pCpsCD) fusion in R6, an unencapsulated *S. pneumoniae* strain, no obvious effect on growth or lysis was evident (data not shown). It is possible that absence of the transmembrane section of this protein results in a protein unable to undergo normal localization. Furthremore, the absence of capsule, and thus the hyper-sensitivity to LytA may make seeing affects difficult. Alternatively, other as yet unidentified BY-kinases are present which may affect the phosphorylation of the LytA. We are currently undertaking further studies to investigate this in more detail.

To date, no phosphoproteome of the pneumococcus has concentrated on the discovery of solely tyrosine phosphorylated proteins. Indeed, the original phosphoproteomic study on the pneumococcus only found 12 proteins phosphorylated on tyrosine, although suprisingly auto-phosphorylating tyrosine kinase CpsD was not amongst these (Sun *et al.*, 2010). Thus, this would suggest that this study likely did not find the majority of tyrosine phosphorylated proteins. Indeed, a recent study which concentrated solely on finding phosphorylated tyrosines in *E. coli,* took the number of proteins known to be tyrosine phosphorylated in the bacteria from 32 to 342 (Hansen *et al.*, 2013), suggestive that tyrosine phosphorylation is a likely much under-appreciated form of post-translational regulation in bacteria as a whole, including *S. pneumoniae*. With this study illustrating that tyrosine phosphorylation can influence the activity of a major virulence factor this suggests that tyrosine phosphorylation could be a much more important form of post-translational regulation than is to date recognized.

Acknowledgements

We would like to thank Prof Jeffrey Weiser for supply of the Janus cassette and Professor James Paton for supply of LytA expressing vector, pGL80.

This study was funded by NHMRC project Grant 1048749 to RM and AS.

Table 1.

Strain	**Reference**
E. coli	
DH5α	Gibco-BRL
Plasmid	
pGL80	(Garcia *et al.*, 1986)
pAL2	(Trappetti *et al.*, 2011)
pCpsCD	This work
$pGL80_{Y264F}$	This work
$pGL80_{Y264E}$	This work
$pGL80_{Y264A}$	This work
S. pneumoniae	
D39S	This work
D39 LytAJanus	This work
D39 $LytA_{Y264F}$	This work
D39 $LytA_{Y264E}$	This work
D39 $LytA_{Y264N}$	This work
Oligonucleotide	**Sequence**
AS95	5’ CTGGGTCAAGTTCAAGGACACTTGG 3’
AS96	5’ CCAAGTGTCCTTGAACTTGACCCAG 3’
AS97	5’ CTGGGTCAAGGAAAAGGACACTTGG 3’
AS98	5’ CCAAGTGTCCTTTTCCTTGACCCAG 3’
AS99	5’ CTGGGTCAAGGCAAAGGACACTTGG 3’
AS100	5’ CCAAGTGTCCTTTGCCTTGACCCAG 3’
AS91	5’ ACAGGAGGACTCTCTatgGACACCCGTGTGAAACGTCCT 3’
AS92	5’ GCGCGAATTcttaCTATTTTTTATTTTTCCCGTAATCTCC 3’
AS101	5’ TTGACTGTCCTTATTTCATTCCGC 3’
AS102	5’ CCTCTCACATTACCCTACATATCG 3’
AS1	5’ GCggtaccagGATACTCGTGTGAAACGTCCGG 3’
AS2	5’ taatgtcggcatTTTCAACTTACCCAAGTTTGGCAC 3’
AS3	5’ ggtaagttgaaaATGCCGACATTAGAAATAGCACAA 3’
AS4	5’ GCgagctcTTATTTTTTACCATAATTTCCATAGGA 3’
AS68	5’ ACAGGAGGACTCTCTATGGATACTCGTGTGAAACGTCCGG 3’
AS77	5’ GCGCGAATTTTATTTTTTACCATAATTTCCATAGGA 3’
AS113	5’ CCGTTTGATTTTTAATGGATAATG 3’
AS114	5’ AGAGACCTGGGCCCCTTTCC 3’
AS117	5’ CATTATCCATTAAAAATCAAACGGATTCTACTCCTTATCAATTAAAACAAC 3’
AS118	5’ GGAAAGGGGCCCAGGTCTCTTAATGGAATGTCTTTCAAATCAGAACAG 3’
AS120	5’ TGTTCCCAGCTATTTTTATTCAGA 3’
AS121	5’ TCTCTTTATCCCCTTTCCTTATGC 3’

References

Beard, S. J., Salisbury, V., Lewis, R. J., Sharpe, J. A. & MacGowan, A. P. (2002). Expression of lux genes in a clinical isolate of *Streptococcus pneumoniae*: using bioluminescence to monitor gemifloxacin activity. *Antimicrob Agents Chemother* **46**, 538-542.

Bender, M. H. & Yother, J. (2001). CpsB is a modulator of capsule-associated tyrosine kinase activity in *Streptococcus pneumoniae*. *J Biol Chem* **276**, 47966-47974.

Berry, A. M. & Paton, J. C. (2000). Additive attenuation of virulence of *Streptococcus pneumoniae* by mutation of the genes encoding pneumolysin and other putative pneumococcal virulence proteins. *Infect Immun* **68**, 133-140.

Byrne, J. P., Morona, J. K., Paton, J. C. & Morona, R. (2011). Identification of *Streptococcus pneumoniae* Cps2C Residues That Affect Capsular Polysaccharide Polymerization, Cell Wall Ligation, and Cps2D Phosphorylation. *J Bacteriol* **193**, 2341-2346.

Dalia, A. B. & Weiser, J. N. (2011). Minimization of bacterial size allows for complement evasion and is overcome by the agglutinating effect of antibody. *Cell Host Microbe* **10**, 486-496.

De Las Rivas, B., Garcia, J. L., Lopez, R. & Garcia, P. (2002). Purification and polar localization of pneumococcal LytB, a putative endo-beta-N-

acetylglucosaminidase: the chain-dispersing murein hydrolase. *J Bacteriol* **184**, 4988-5000.

Eldholm, V., Johnsborg, O., Haugen, K., Ohnstad, H. S. & Havarstein, L. S. (2009). Fratricide in *Streptococcus pneumoniae*: contributions and role of the cell wall hydrolases CbpD, LytA and LytC. *Microbiology* **155**, 2223-2234.

Ericsson, D. J., Standish, A., Kobe, B. & Morona, R. (2012). Wzy-dependent bacterial capsules as potential drug targets. *Curr Drug Targets* **13**, 1421-1431.

Fernandez-Tornero, C., Lopez, R., Garcia, E., Gimenez-Gallego, G. & Romero, A. (2001). A novel solenoid fold in the cell wall anchoring domain of the pneumococcal virulence factor LytA. *Nat Struct Biol* **8**, 1020-1024.

Fernandez-Tornero, C., Garcia, E., Lopez, R., Gimenez-Gallego, G. & Romero, A. (2002). Two new crystal forms of the choline-binding domain of the major pneumococcal autolysin: insights into the dynamics of the active homodimer. *J Mol Biol* **321**, 163-173.

Fernebro, J., Andersson, I., Sublett, J., Morfeldt, E., Novak, R., Tuomanen, E., Normark, S. & Normark, B. H. (2004). Capsular expression in *Streptococcus pneumoniae* negatively affects spontaneous and antibiotic-induced lysis and contributes to antibiotic tolerance. *J Infect Dis* **189**, 328-338.

Garcia, E., Garcia, J. L., Ronda, C., Garcia, P. & Lopez, R. (1985). Cloning and expression of the pneumococcal autolysin gene in *Escherichia coli*. *Mol Gen Genet* **201**, 225-230.

Garcia, P., Garcia, J. L., Garcia, E. & Lopez, R. (1986). Nucleotide sequence and expression of the pneumococcal autolysin gene from its own promoter in *Escherichia coli*. *Gene* **43**, 265-272.

Giudicelli, S. & Tomasz, A. (1984). Attachment of pneumococcal autolysin to wall teichoic acids, an essential step in enzymatic wall degradation. *J Bacteriol* **158**, 1188-1190.

Goebel, W. F. & Avery, O. T. (1929). A Study of Pneumococcus Autolysis. *J Exp Med* **49**, 267-286.

Hansen, A. M., Chaerkady, R., Sharma, J. & other authors (2013). The *Escherichia coli* phosphotyrosine proteome relates to core pathways and virulence. *PLoS Pathog* **9**, e1003403.

Henriques, M. X., Rodrigues, T., Carido, M., Ferreira, L. & Filipe, S. R. (2011). Synthesis of capsular polysaccharide at the division septum of *Streptococcus pneumoniae* is dependent on a bacterial tyrosine kinase. *Mol Microbiol* **82**, 515-534.

Kelley, L. A. & Sternberg, M. J. (2009). Protein structure prediction on the Web: a case study using the Phyre server. *Nat Protoc* **4**, 363-371.

Laemmli, U. K. (1970). Cleavage of structural proteins during the assembly of the head of bacteriophage T4. *Nature* **227**, 680-685.

Martner, A., Dahlgren, C., Paton, J. C. & Wold, A. E. (2008). Pneumolysin released during Streptococcus pneumoniae autolysis is a potent activator of intracellular oxygen radical production in neutrophils. *Infect Immun* **76**, 4079-4087.

McAllister, L. J., Tseng, H. J., Ogunniyi, A. D., Jennings, M. P., McEwan, A. G. & Paton, J. C. (2004). Molecular analysis of the psa permease complex of *Streptococcus pneumoniae*. *Mol Microbiol* **53**, 889-901.

Mellroth, P., Daniels, R., Eberhardt, A., Ronnlund, D., Blom, H., Widengren, J., Normark, S. & Henriques-Normark, B. (2012). LytA, major autolysin of *Streptococcus pneumoniae*, requires access to nascent peptidoglycan. *J Biol Chem* **287**, 11018-11029.

Mellroth, P., Sandalova, T., Kikhney, A. & other authors (2014). Structural and functional insights into peptidoglycan access for the lytic amidase LytA of Streptococcus pneumoniae. *mBio* **5**, e01120-01113.

Morona, J. K., Paton, J. C., Miller, D. C. & Morona, R. (2000). Tyrosine phosphorylation of CpsD negatively regulates capsular polysaccharide biosynthesis in *Streptococcus pneumoniae*. *Mol Microbiol* **35**, 1431-1442.

Morona, J. K., Morona, R., Miller, D. C. & Paton, J. C. (2002). *Streptococcus pneumoniae* capsule biosynthesis protein CpsB is a novel manganese-dependent phosphotyrosine-protein phosphatase. *J Bacteriol* **184**, 577-583.

Morona, J. K., Miller, D. C., Morona, R. & Paton, J. C. (2004). The effect that mutations in the conserved capsular polysaccharide biosynthesis genes *cpsA*, *cpsB*, and *cpsD* have on virulence of *Streptococcus pneumoniae*. *J Infect Dis* **189**, 1905-1913.

Morona, J. K., Morona, R. & Paton, J. C. (2006). Attachment of capsular polysaccharide to the cell wall of *Streptococcus pneumoniae* type 2 is required for invasive disease. *Proc Natl Acad Sci U S A* **103**, 8505-8510.

Morona, R., van den Bosch, L. & Manning, P. A. (1995). Molecular, genetic, and topological characterization of O-antigen chain length regulation in *Shigella flexneri*. *J Bacteriol* **177**, 1059-1068.

Olivares-Illana, V., Meyer, P., Bechet, E. & other authors (2008). Structural basis for the regulation mechanism of the tyrosine kinase CapB from *Staphylococcus aureus*. *PLoS Biol* **6**, e143.

Romero, P., Lopez, R. & Garcia, E. (2007). Key role of amino acid residues in the dimerization and catalytic activation of the autolysin LytA, an important virulence factor in Streptococcus pneumoniae. *J Biol Chem* **282**, 17729-17737.

Rosenow, C., Ryan, P., Weiser, J. N., Johnson, S., Fontan, P., Ortqvist, A. & Masure, H. R. (1997). Contribution of novel choline-binding proteins to adherence, colonization and immunogenicity of Streptococcus pneumoniae. *Mol Microbiol* **25**, 819-829.

Sanz, J. M., Lopez, R. & Garcia, J. L. (1988). Structural requirements of choline derivatives for 'conversion' of pneumococcal amidase. A new single-step procedure for purification of this autolysin. *FEBS Lett* **232**, 308-312.

Soulat, D., Jault, J. M., Duclos, B., Geourjon, C., Cozzone, A. J. & Grangeasse, C. (2006). *Staphylococcus aureus* operates protein-tyrosine phosphorylation through a specific mechanism. *J Biol Chem* **281**, 14048-14056.

Standish, A. J., Stroeher, U. H. & Paton, J. C. (2005). The two-component signal transduction system RR06/HK06 regulates expression of *cbpA* in *Streptococcus pneumoniae*. *Proc Natl Acad Sci U S A* **102**, 7701-7706.

Standish, A. J., Salim, A. A., Zhang, H., Capon, R. J. & Morona, R. (2012). Chemical inhibition of bacterial protein tyrosine phosphatase suppresses capsule production. *PLoS ONE* **7**, e36312.

Standish, A. J., Salim, A. A., Capon, R. J. & Morona, R. (2013). Dual inhibition of DNA polymerase PolC and protein tyrosine phosphatase CpsB uncovers a novel antibiotic target. *Biochem Biophys Res Commun* **430**, 167-172.

Standish, A. J. & Morona, R. (2014). The role of bacterial protein tyrosine phosphatases in the regulation of the biosynthesis of secreted polysaccharides. *Antioxid Redox Signal* **20**, 2274-2289.

Sun, X., Ge, F., Xiao, C. L., Yin, X. F., Ge, R., Zhang, L. H. & He, Q. Y. (2010). Phosphoproteomic analysis reveals the multiple roles of phosphorylation in pathogenic bacterium *Streptococcus pneumoniae*. *J Proteome Res* **9**, 275-282.

Sung, C. K., Li, H., Claverys, J. P. & Morrison, D. A. (2001). An rpsL cassette, janus, for gene replacement through negative selection in Streptococcus pneumoniae. *Appl Environ Microbiol* **67**, 5190-5196.

Tomasz, A. & Westphal, M. (1971). Abnormal autolytic enzyme in a pneumococcus with altered teichoic acid composition. *Proc Natl Acad Sci U S A* **68**, 2627-2630.

Trappetti, C., Potter, A. J., Paton, A. W., Oggioni, M. R. & Paton, J. C. (2011). LuxS mediates iron-dependent biofilm formation, competence, and fratricide in Streptococcus pneumoniae. *Infect Immun* **79**, 4550-4558.

Whitmore, S. E. & Lamont, R. J. (2012). Tyrosine phosphorylation and bacterial virulence. *Int J Oral Sci* **4**, 1-6.

Figures

Figure 1. Location of Y264 in Choline Binding Repeat of the Choline Binding Domain of LytA. (a) Choline Binding Repeats of LytA (D39; SPD_1737) showing site of tyrosine phosphorylation (Y264) present in ChBR4. While there is significant similarity between repeats, Y264 is the only tyrosine present at this site. (b) Illustration of the position of Y264 (Red) within the structure of the choline binding domain of LytA (Pdb: 1GVM) (Fernandez-Tornero *et al.*, 2002). Bound choline residue is highlighted in green.

Figure 2. BY-kinase CpsD and PTP CpsB act on LytA. (a) Whole cell lysates from *E. coli* DH5α without (1) and with (2) expression of pCpsCD was investigated for tyrosine phosphorylation via Western immunoblotting. CpsCD is marked, while other proteins are additional increases in phosphorylation. (b) LytA (0.1 µg) purified either without (lane 1) or with (lane 2) co-expression of an active form of CpsD (pCpsCD) and (lane 3) $LytA_{Y264F}$ co-expressed with CpsD were investigated for tyrosine phosphorylation via Western immunoblotting (αPY). Loading was confirmed by Coomassie Brilliant Blue stained SDS-PAGE. (c) CpsB (2 µg) was incubated alone (lane 1) or with LytA (1 µg) (lane 2) for 1 hr and phosphorylation was investigated by Western immunobloting with αPY and αLytA.

Figure 3. LytA phosphorylation increases attachment to DEAE. (a) 10 µg of soluble protein from *E. coli* DH5α containing (lane 1) LytA, (lane 2) LytA-P and (lane 3) $LytA_{Y264F}$-P were separated on SDS-PAGE gel, and subjected to Western immunoblotting with αLytA. (b) 0.2 mg/ml of each soluble lysate was incubated with DEAE-Sepharose for 30 min as described in Material and Methods, with bound

protein detected by Coomassie Brilliant Blue staining of the SDS-PAGE gel. Dilutions of bound proteins samples were electrophoresed (Neat, 1:2 and 1:4) in order to help estimate differences. (c) Differences were quantified by Image J densitometric analysis of result from 3 separate experiments. (* - $p < 0.05$, One-way Anova with a Tukey Test).

Figure 4. $LytA_{Y264E}$ has increased attachment to DEAE. (a) 10 µg of soluble protein from E. coli DH5α containing (lane 1) LytA, (lane 2) $LytA_{Y264E}$ and (lane 3) $LytA_{Y264A}$ were separated on SDS-PAGE gel, and subjected to Western immunoblotting with αLytA. (b) 0.2 mg/ml of each soluble lysate was incubated with DEAE-Sepharose for 30 min as described in Material and Methods, with bound protein detected by Coomassie Brilliant Blue staining of the SDS-PAGE gel. Dilutions of bound proteins samples were electrophoresed (Neat, 1:2) in order to help estimate differences. (c) Differences were quantified by Image J densitometric analysis of result from 3 separate experiments (*** - $p < 0.001$, ** - $p < 0.01$, One-way Anova with a Tukey Test).

Figure 5. Phosphorylation influences LytA dimerization. (a) LytA (lanes 1 & 5) and it variants $LytA_{Y264F}$ (lanes 2 & 6), $LytA_{Y264E}$ (lanes 3& 7) and $LytA_{Y264A}$ (lanes 4 & 8) were purified, dialyzed as described in Materials and Methods, and approximately 2 µg separated by non-dentaturing PAGE. (b) Relative percentages of the monomer present were determined by Image J densitometric anaylsis of result from 3 separate experiments (* - $p < 0.05$, One-way Anova with a Tukey Test). (c) Dialysed samples were also separated on denaturing SDS-PAGE, and stained with Coomassie Brilliant Blue. Molecular weights (MW) are indicated in kDa.

716

717 **Figure 6. Phosphorylation increases LytA amidase activity**. (a) Purified proteins (2
718 µg/ml) or (b) cell lysates (250 µg/ml) containing (1) LytA, (2) LytA-P, (3)$LytA_{Y264F-P}$,
719 (4) $LytA_{Y264E}$ and (5) $LytA_{Y264A}$ were compared for LytA amidase activity using a
720 turbidometric assay as described in Materials and Methods. Results represent Mean ±
721 SD from 2 (purified proteins) and 3 (cell lysates) independent experiments
722 respectively. Statistical analysis was undertaken using a One-way Anova with a
723 Tukey Test (**** - $p < 0.0001$; ** - $p < 0.01$).

724

725 **Figure 7. Chromosomal LytA phosphoablative and phosphomimetic**
726 **substitutions alter D39 autolysis.** (a) Lysates from D39, D39 $LytA_{Y264F}$, D39
727 $LytA_{Y264E}$ and D39 $LytA_{Y264A}$ were separated on SDS-PAGE gel and subjected to
728 Western immunoblotting with αLytA and αCpsB. (b) Strains D39, D39LytAJanus,
729 D39 $LytA_{Y264F}$, D39 $LytA_{Y264E}$ and D39 $LytA_{Y264A}$ were grown for indicated time
730 periods in C+Y with A_{600} recorded every 30 mins. Result is representative of four
731 separate experiments. (c) Rate of autolysis was compared as described in Material and
732 Methods. Statistical analysis was undertaken using a One-way Anova with a Tukey
733 Test (*** - $p < 0.001$).

(a)

```
         1          10          20
ChBR1   H.SDGSYPKD..KFEKI.NG.TWYYF
ChBR2   D.SSGYMLAD..RWRKHTDG.NWYWF
ChBR3   D.NSGEM.AT..GWKKIAD..KWYYF
ChBR4   N.EEGAM.KT..GWVKYKD..TWYYL
ChBR5   DAKEGAMVSN..AFIQSADGTGWYYL
ChBR6   K.PDGTL.ADRPEFTVEPDG.LITVK
```

(b)

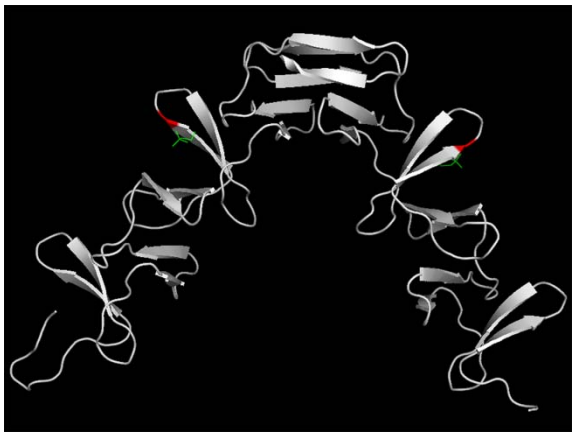

Figure 1

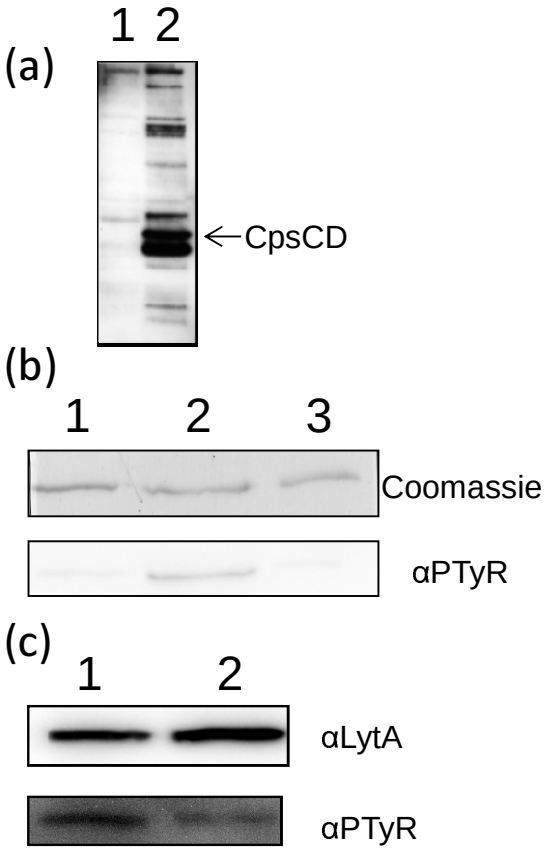

Figure 2

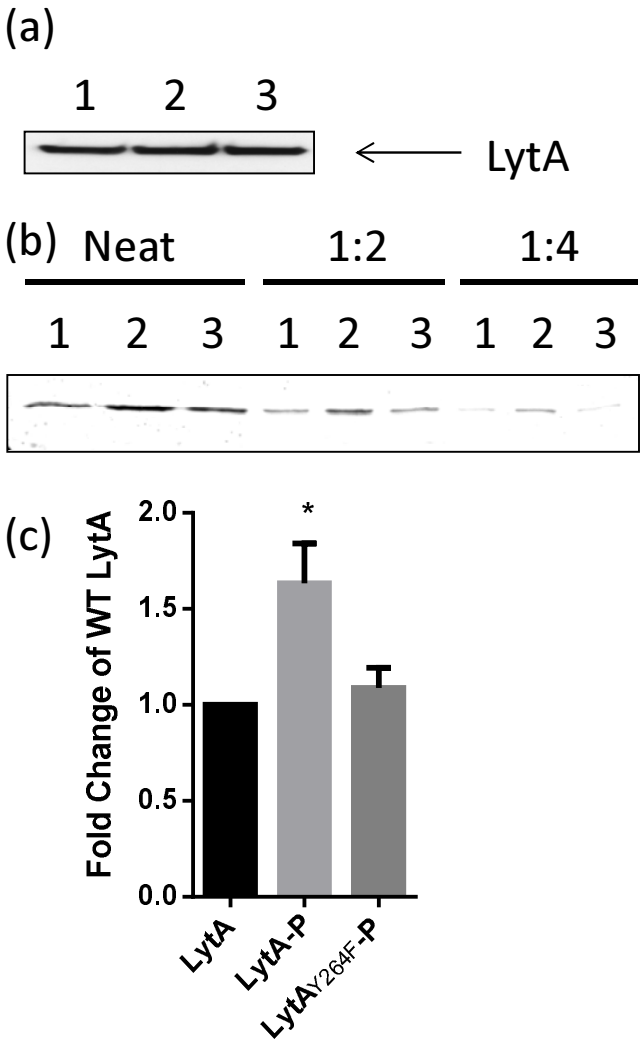
(a)
1 2 3
LytA
(b) Neat 1:2 1:4
1 2 3 1 2 3 1 2 3
(c)
Fold Change of WT LytA
2.0
1.5
1.0
0.5
0.0
*
LytA
LytA-P
LytAY264F-P

Figure 3

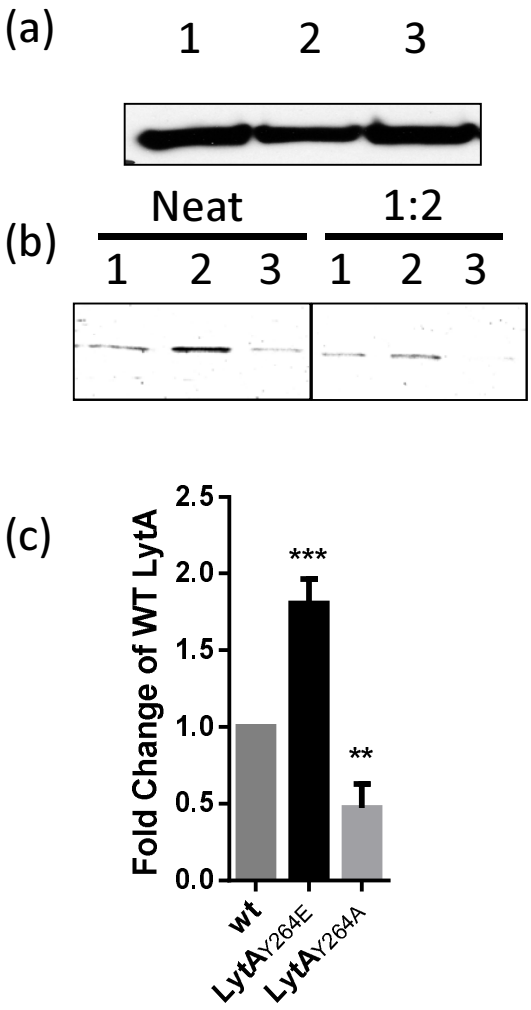
(a)
1
2
3
(b)
Neat
1:2
1 2 3 1 2 3
(c)
Fold Change of WT LytA
2.5
2.0
1.5
1.0
0.5
0.0
***
**
wt
LytA Y264E
LytA Y264A

Figure 4

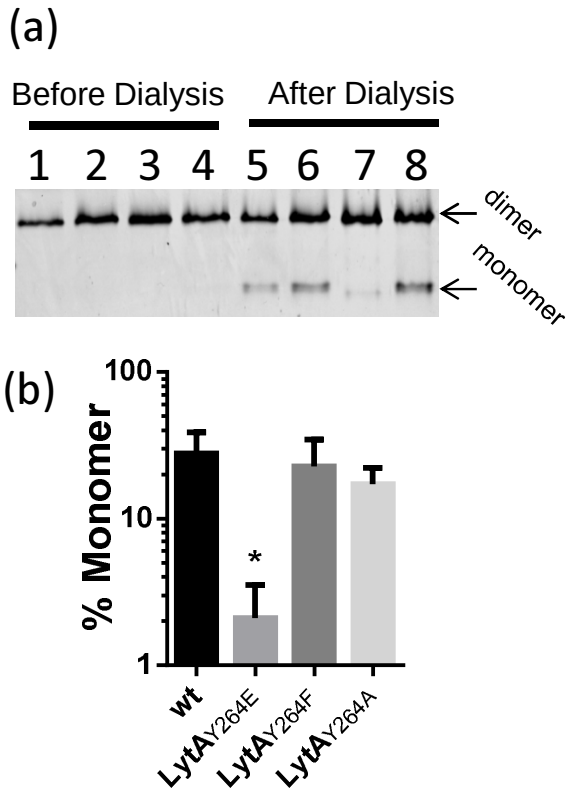
(a)
Before Dialysis
After Dialysis
1 2 3 4 5 6 7 8
dimer
monomer
(b)
% Monomer
100
10
1
*
wt
LytA Y264E
LytA Y264F
LytA Y264A
(c)
MW 1 2 3 4
45
30
20

Figure 5

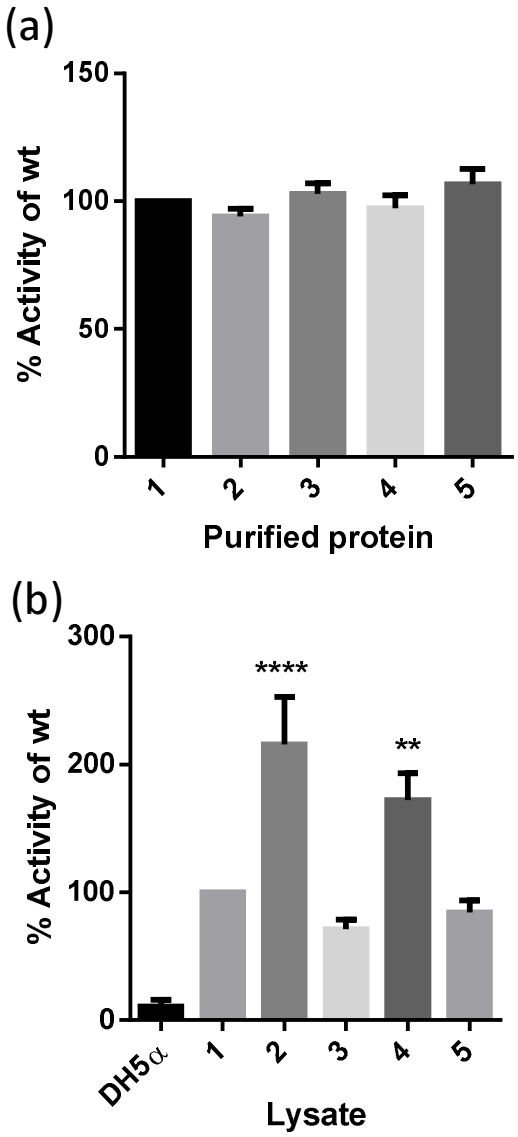
(a)
150
100
50
0
% Activity of wt
1
2
3
4
5
Purified protein
(b)
300
200
100
0
% Activity of wt
****
**
DH5α
1
2
3
4
5
Lysate

Figure 6

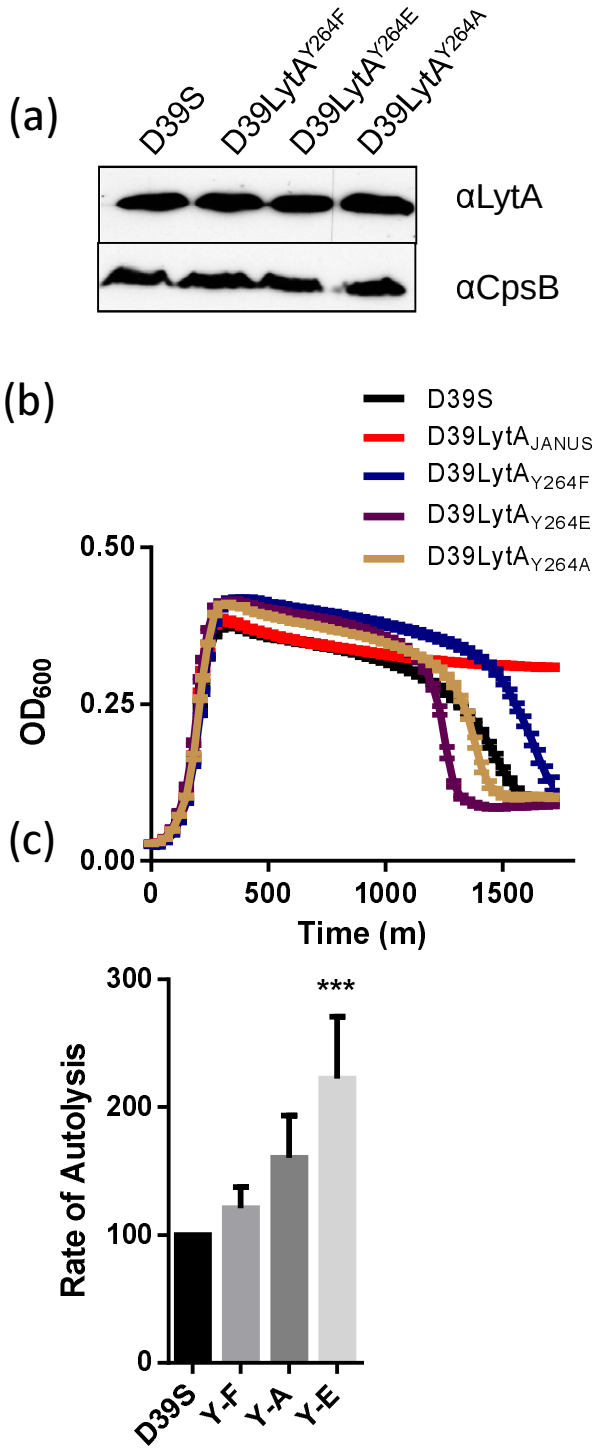
(a)
D39S
D39LytA Y264F
D39LytA Y264E
D39LytA Y264A
αLytA
αCpsB
(b)
D39S
D39LytA JANUS
D39LytA Y264F
D39LytA Y264E
D39LytA Y264A
OD600
0.50
0.25
0.00
0
500
1000
1500
Time (m)
(c)
Rate of Autolysis
300
200
100
0
***
D39S
Y-F
Y-A
Y-E

Figure 7